Malaysian Journal of Analytical Sciences (MJAS)
Published by Malaysian Analytical Sciences Society

PREPARATION AND ADSORPTION STUDIES OF MOLECULARLY IMPRINTED POLYMER FOR SELECTIVE RECOGNITION OF TRYPTOPHAN

(Penyediaan dan Kajian Penjerapan Polimer Molekul Tercetak untuk Pengecaman Selektif Triptofan)

Nur Habibah Safiyah Jusoh[1], Faizatul Shimal Mehamod[2]*, Noor Fadilah Yusof[3], Abd Mutalib Md Jani[4], Faiz Bukhari Mohd Suah[5], Marinah Mohd Ariffin[1], Nur Asyiqin Zulkefli[1]

[1]*Faculty of Science and Marine Environment*
[2]*Advanced Nano Materials (ANoMA) Research Group, Faculty of Science and Marine Environment*
Universiti Malaysia Terengganu, 21030 Kuala Nerus, Terengganu, Malaysia
[3]*School of Chemical and Energy Engineering, Faculty of Engineering,*
Universiti Teknologi Malaysia, 81310 Skudai, Johor Bahru, Malaysia.
[4]*Faculty of Applied Sciences,*
Universiti Teknologi MARA, Perak Branch, Tapah Campus, 35400 Perak, Malaysia
[5]*School of Chemical Sciences,*
Universiti Sains Malaysia, 11800 Minden, Pulau Pinang, Malaysia

**Corresponding author: fshimal@umt.edu.my*

Received: 13 September 2021; Accepted: 18 December 2021; Published: 28 April 2022

Abstract

One of the effective technologies in molecular recognition is based on the molecular imprinting process. In this work, the polymers were prepared by bulk polymerization, using methacrylic acid and ethylene glycol dimethacrylate as the functional monomer and crosslinking agent, respectively. The polymers were characterized by Fourier transform infrared spectroscopy, scanning electron microscopy and surface area and porosity analyses. Several parameters influencing the adsorption efficiency of Tryptophan (Tryp) such as adsorbent dosage, contact time, pH of sample solution as well as selectivity and reproducibility study, have been evaluated. The Tryptophan-imprinted polymer (Tryp-IP) showed significantly higher removal efficiency and selective binding capacity towards Tryp compared to non-imprinted polymer (NIP). The adsorption isotherm demonstrated that the Tryp-IP followed Langmuir isotherm model, indicating the Tryp-IP owning the homogenous surface type of adsorbent. In contrast, the NIP fit with the Redlich-Peterson model, indicating that mechanism adsorption is a mixed type. The kinetic study revealed that pseudo-second order was the appropriate kinetic model for Tryp-IP and the adsorption kinetic of NIP appeared to fit with pseudo-first order.

Keywords: molecularly imprinted polymer, tryptophan, adsorption study

Abstrak

Salah satu teknologi yang efektif dalam pengecaman molekul adalah berdasarkan proses pencetakan molekul. Dalam kajian ini, polimer telah disediakan melalui pempolimeran pukal, masing-masing menggunakan asid metakrilik dan etilena glikol dimetakrilat sebagai monomer berfungsi dan agen tautsilang. Polimer dicirikan oleh spektroskopi inframerah transformasi Fourier, pengimbasan mikroskop elektron dan analisis luas permukaan dan keliangan. Beberapa parameter yang mempengaruhi kecekapan penjerapan Triptofan (Tryp) seperti dos penjerap, masa sentuhan, pH larutan sampel serta kajian selektiviti dan kebolehulangan telah dinilai. Polimer tercetak-

Triptofan (Tryp-IP) menunjukkan kecekapan penyingkiran dan kapasiti pengikatan yang lebih tinggi terhadap Tryp berbanding polimer tidak dicetak (NIP). Isoterma penjerapan menunjukkan bahawa Tryp-IP mematuhi model isoterma Langmuir, ini menunjukkan Tryp-IP memiliki jenis penjerap permukaan homogen. Sebaliknya, NIP mematuhi model Redlich-Peterson, menunjukkan mekanisme penjerapan adalah jenis campuran. Kajian kinetik mendedahkan bahawa tertib pseudo-kedua adalah model kinetik yang sesuai untuk Tryp-IP dan kinetik penjerapan NIP kelihatan lebih sesuai dengan tertib pseudo-pertama.

Kata kunci: polimer tercetak molekul, triptofan, kajian penjerapan

Introduction

Tryptophan (Tryp) is one of the essential amino acids that is necessary for normal growth and it also acts as a precursor for several bioactive compounds such as nicotinamide (vitamin B6), serotonin, melatonin, tryptamine, kynurenine, and xanthurenic acids [1]. Tryp cannot be synthesized in the human body. However, it can be supplied via our dietary intake such as high protein food and fiber rich food like banana, soy, egg and rice. Even though the Tryp in the human body is relatively low, its potency is very significant. It is one of the amino acids capable of passing through the blood- brain barrier, which makes it very important for protein synthesis in our body [2]. Previous studies have shown that Tryp deficiency in the body can affect mood or cause depressive symptoms, whereas low serotonin levels contribute to increased anxiety and depression [3]. Since Tryp acts as a precursor for serotonin synthesis, the level of serotonin depends on the concentration of Tryp in the body [4]. From this point of view, it is crucial to determine the level of Tryp in the body to monitor this condition. At present, many technologies have been applied for the determination of Tryp, such as electrochemical sensors [5], high-performance liquid chromatography (HPLC) [6], solid-phase extraction-liquid chromatographic-tandem mass spectrometric (XLC-MS/MS) [7] and tandem mass spectrometer [8]. These techniques are very selective and precise; however, they often require pre-treatment steps, expensive and complicated instruments, skilled operators and a lot more time [9]. For these reasons, attention has been focused on the adsorption method due to its low cost and ease of operation. The latest development of adsorbent material for the determination and removal of Tryp/ Tryp derivatives such as polymeric resin [10], gold nanoparticles [11] and activated carbon [12], has shown outstanding results for the adsorptive capacity of Tryp.

In recent years, the low-cost adsorbent materials fabricated from molecular imprinting technology have attracted much attention due to the high selectivity and simple preparation method, which gives the technology a broad range of applications. Molecularly imprinted polymer (MIP) is an adsorbent from the imprinting technique with specific binding sites, shape and size towards the imprinted analyte called template. The molecular imprinting technique is a process that involves the polymerization reaction of functional monomers with the template molecule, thus allowing the formation of polymer networks to possess binding sites complementary with the template molecule [13]. MIP has several advantages which include low cost, ease of preparation, high stability and high selectivity and affinity. In addition, MIP is an insoluble substance with high durability under extreme pH conditions, organic solvents and high temperatures [14]. In general, many researchers favored the non-covalent approach due to the straightforward procedure, easy template removal as well as the fact that imprinted polymer can be used in various applications because most of the biomolecular interaction were non-covalent bond [15]. During pre-polymerization, functional monomers and template interaction are formed by self-assembly *via* non-covalent interactions, such as hydrogen bond, ionic interaction, hydrophobic interaction, and Van der Waals interaction [16]. Therefore, the present work highlights the application of MIP as a versatile material for selective determination of Tryp molecule. Tryptophan-imprinted polymer designated as Tryp-IP was prepared by bulk polymerization. Figure 1 shows a schematic for the formation of MIP for Tryp *via* the imprinting technique. The process involves methacrylic acid (MAA), ethylene glycol dimethacrylate (EGDMA) and azobisisobutyronitrile (AIBN) as the functional monomer, cross-linker and initiator, respectively. Once

the polymerization is complete, the removal of the template from the polymer matrix, leaves the cavities that are ideally complementary in terms of size, shape, and function to the template analyte. The corresponding non-imprinted polymer (NIP) was synthesized as a control sample.

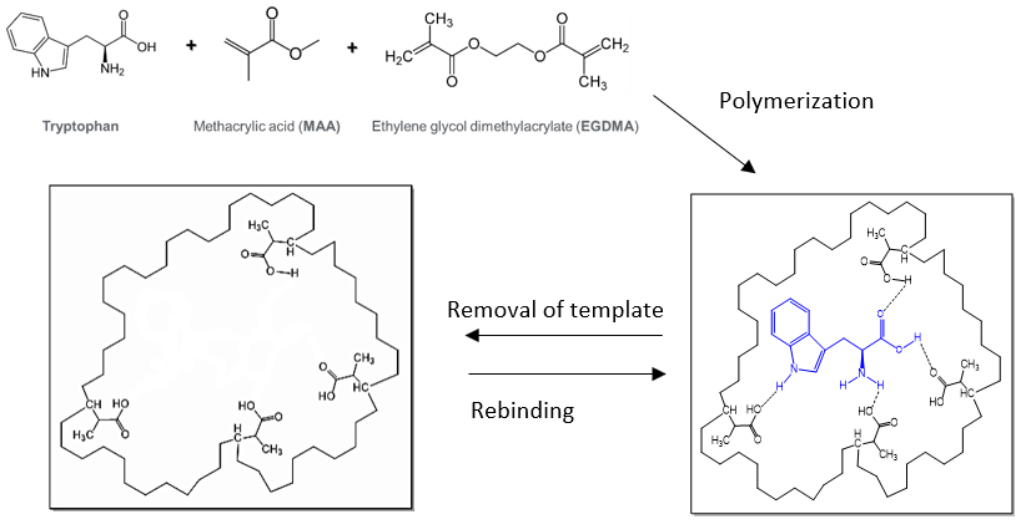

Figure 1. Schematic of the molecular imprinting process for Tryp

Materials and Methods

Materials

Tryptophan (Tryp), kynurenine (Kyn), tyrosine (Tyr), phenylalanine (Phe), methacrylic acid (MAA), ethylene glycol dimethacrylate (EGDMA), and azobisisobutyronitrile (AIBN) were purchased from Sigma Aldrich, Germany whereas methanol, acetic acid, sodium hydroxide (NaOH), hydrochloric acid (HCl) were supplied by R&M Chemicals, UK.

Preparation of Tryp-imprinted polymer

The preparation of Tryp-IP was carried out by the bulk polymerization method [17, 18]. Initially, Tryptophan (Tryp, 1 mmol) was dissolved in water/methanol (1:3 v/v). Then the functional monomer (MAA, 10 mmol), cross-linker (EGDMA, 30 mmol) and initiator; (AIBN) were added into the glass tube to allow the polymerization process to occur. Then, the mixture was stirred until homogeneous and purged with nitrogen gas before being placed in an oil bath at 60 °C for 48 hours. Upon completion of the polymerization reaction, the polymers obtained were crushed, ground, and sieved. The polymers were treated with methanol and acetic acid in a 9:1 v/v ratio by Soxhlet extraction to remove the template molecules. The obtained polymers were stored at room temperature for further characterization. Finally, the non-imprinted polymer (NIP) as a control sample was prepared using the same method but in the absence of the template.

Characterization of the polymers

The polymers were characterized by attenuated total reflection-Fourier transform infrared spectroscopy (ATR-FTIR). The spectra were recorded from 500 cm^{-1} to 4000 cm^{-1}. Then, the surface morphology of polymers was observed by Scanning Electron Microscopy (SEM). Each polymer was mounted on the stubs and coated with gold for protection from the electron beam. Next, the determination of the specific surface area, pore volume and pore diameter were performed by porosity analyzer using Bruner-Emmett-Teller (BET) and Barrett-Joyner-Halenda (BJH) technique.

Adsorption studies

The adsorption studies were conducted by batch rebinding experiment, which was performed in an aqueous medium [19]. First, 1 ppm of Tryp solution was prepared and mixed with a different mass of Tryp-IP (1, 3, 5, 7, 9 mg) while maintaining other parameters at optimal conditions. After the adsorption process, the Tryp solution was analyzed using a UV-Vis spectrometer to determine the remaining Tryp molecule by observing its final concentration. Then, the percentage removal and adsorption capacity of Tryp-IP towards Tryp was calculated using equations (1) and (2), respectively [20]:

$$\% \text{ removal} = \frac{C_i - C_f}{C_i} \times 100 \quad (1)$$

$$Q_e = \frac{(C_i - C_f)V}{W} \quad (2)$$

In the equations above, C_i and C_f are initial and final concentrations (mg/L) of Tryp solutions, respectively, Q_e (mg/g) is the quantity of total adsorption of Tryp molecules, V (L) is the volume of the solution and W (g) is the weight of polymers.

The interaction and adsorption mechanism of Tryp-IP and Tryp were further studied by fitting equilibrium data into the isotherm models. The adsorption equilibrium data obtained were fitted into Langmuir, Freundlich and Redlich-Peterson isotherm models. Langmuir isotherm is often associated with adsorption on the surface of homogeneous sites within the adsorbent and occurs in a monolayer pattern. Nevertheless, Freundlich isotherms apply to adsorption processes that occur on heterogeneous surfaces. Redlich-Peterson isotherm is a three-parameter isotherm which combines Langmuir and Freundlich isotherms. The Langmuir, Freundlich and Redlich-Peterson equation can be written in the following linear form as stated in equations (3), (4) and (5), respectively [21].

$$\frac{C_e}{Q_e} = \frac{1}{BQ_o} + \frac{C_e}{B} \quad (3)$$

$$\ln Q_e = \ln K_F + \frac{1}{n} \ln C_e \quad (4)$$

$$\ln \frac{C_e}{Q_e} = \beta \ln C_e - \ln A \quad (5)$$

In equations (3), (4) and (5), Q_e is the equilibrium adsorption capacity (mg/g), C_e is the equilibrium concentration of adsorbents at equilibrium (mg/L), and Q_o is the maximum adsorption capacity of the adsorbents (mg/g). B (L/mg) is the Langmuir adsorption constant, while K_F (mg/g) is the Freundlich adsorption equilibrium constants indicating the sorption capacity and 1/n represents the intensity of the adsorption. Meanwhile, A (Lg^{-1}) is Redlich-Peterson isotherm constant and β is the exponent that lies between 0 and 1. The favorability of the Langmuir isotherm was expressed by a dimensionless constant called the separation factor (RL), as shown in equation (6).

$$RL = \frac{1}{1 + B(C_e)} \quad (6)$$

where RL values indicate the adsorption to be unfavorable when RL > 1, linear when RL = 1, favorable when 0 < RL< 1, and irreversible when RL = 0 [21].

Adsorption kinetic study

Adsorption kinetics was studied to determine the kinetic behavior and rate-controlling step for the adsorption process of Tryp-IP. The experiments were conducted using 1 ppm of Tryp solution mixed with 9 mg of Tryp-IP. The kinetics of Tryp uptake by Tryp-IP were analyzed using a UV-Vis spectrometer. The time was set at 0 to 180 min. Two adsorption kinetic models, namely pseudo-first-order and pseudo-second-order, were tested and fitted into the adsorption kinetic data. The pseudo-first and pseudo-second order equations can be expressed in equations (7) and (8), respectively,

$$\ln(q_e - q_t) = \ln q_e - k_1 t \quad (7)$$

$$\frac{t}{q_t} = \frac{1}{k_2 q_e^2} + \frac{t}{q_e} \quad (8)$$

where q_t and q_e (mg/g) represent adsorption capacities at time and equilibrium, respectively, while k_1 and k_2 represent rate constants at equilibrium [22]. Furthermore, the favorability of kinetic models was calculated by standard deviation formula, Δq (%) and relative error, RE (%) as in the following equations:

$$\Delta q(\%) = \sqrt{\frac{[(Q_{e,exp} - q_{e,cal})/Q_{e,exp}]^2}{N-1}} \times 100 \quad (9)$$

$$RE\ (\%) = \frac{|q_{e,cal} - Q_{e,exp}|}{Q_{e,exp}} \times 100 \quad (10)$$

where N is the amount of data points fitted to the plot, $Q_{e,exp}$ and $q_{e,cal}$ (mg/g) are the experimental and calculated adsorption capacities, respectively. A lower Δq (%) gives the desired fitness of polymer to the kinetic model [20].

Effect of pH study

1 ppm of Tryptophan solution was prepared, and the pH was adjusted in the range of 4, 5, 7, 9, 11 and 13, by adding diluted HCl and NaOH. The experiment was carried out by mixing each solution with 9 mg of Tryp-IP. An independent analyte solution was analyzed and the optimum pH for optimum adsorption was determined.

3

Effect of selectivity study

In the selectivity study, the molecular structural analogues of Tryptophan; kynurenine, tyrosine and phenylalanine were tested for the binding performance with Tryp-IP. Firstly, 1 ppm of analyte concentrations were prepared separately and mixed with 9 mg of Tryp-IP. Then, the solutions were analyzed using UV-Vis spectrometer. The distribution coefficient (kd) was calculated based on the equation 11.

$$k_d = \frac{(C_i - C_f)}{C_f}\left(\frac{V}{W}\right) \quad (11)$$

where k_d is the concentration ratio between two solutions, C_i and C_f are initial and final concentrations of each compound, respectively. V (L) is the volume of the solution and W (g) is the weight of polymers [23]. The adsorption capacity of the polymer increases as the value of k_d increases. Selectivity coefficient (k), which indicates the selectivity of Tryp over the competitive compounds was calculated based on the equation 12 below:

$$k = \frac{k_d(\text{Tryp})}{k_d(\text{Kyn/Tyr/Phe})} \quad (12)$$

Relative selectivity coefficient (k') was determined by comparing the ratio of Tryp-IP and NIP as equation 13 below:

$$k' = \frac{k\,(\text{Tryp-IP})}{k\,(\text{NIP})} \quad (13)$$

Reproducibility study

A reproducibility study was explored to evaluate the practical application of the prepared adsorbent. Firstly, 1 ppm of Tryp solution was mixed with nine sets of Tryp-IP (9 mg) at the optimal time taken. Then, each solution was evaluated by UV- Vis spectrometer and its adsorption capacity were calculated.

Results and Discussion

FTIR characterization

Figure 2 shows the FTIR spectra of Tryp, Tryp-IP before and after template removal and the NIP. From the Tryp spectrum in Figure 2(a), a peak at 3400 cm^{-1} and 3012 cm^{-1} were observed, indicating a peak for NH stretching from the indole group and alkene C-H stretching, respectively. The IR peaks obtained at 1654 cm^{-1} and 1575cm^{-1} show the COO- and NH asymmetric stretching vibrations, respectively [9]. Due to the high cross-linking agent, all polymers show similar vibration peaks with almost the same IR spectrum. Based on Figure 2(b), the IR broad peaks obtained around 3471 cm^{-1} – 3275 cm^{-1} show a strong interaction between the NH group of Tryp and the O-H group of the MAA monomer through hydrogen bonding [24]. The aromatic stretching of C-H appeared at 2985 cm^{-1} at a lower intensity indicating the presence of Tryp in the polymer. After removal of Tryp Figure 2(c), the IR spectrum showed the complete disappearance of Tryp characteristic. The intensity of C=O from MAA at 1724 cm^{-1} increased. In comparison with Figure 2(b), the C=O absorption peak shifted from 1716 cm^{-1} to 1724 cm^{-1}, indicating the rupture of the hydrogen bond. In Figure 2(d), the IR spectrum for NIP is expected to be similar to Tryp-IP after the template is removed, where the C-H stretching vibration of MAA appeared at 2985 cm^{-1}. The schematic from Figure 1 is used to confirm all the functional groups present in the polymers for the FTIR spectra.

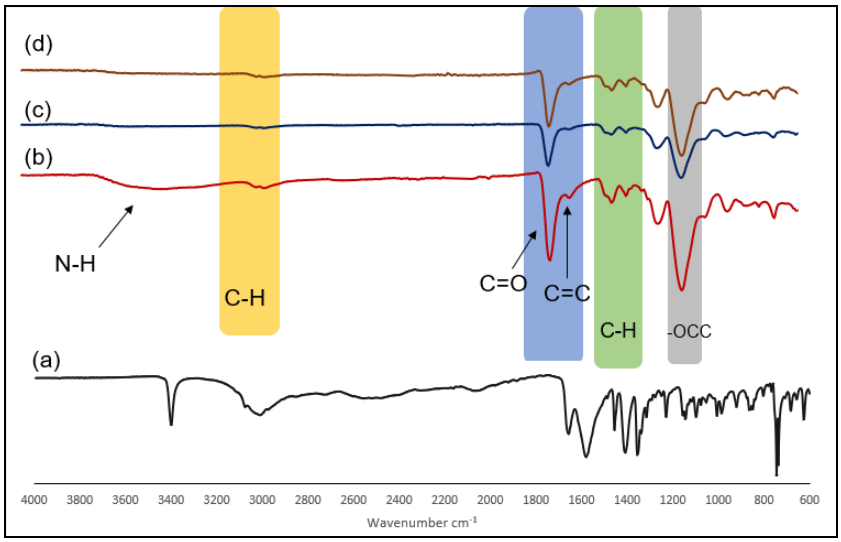

Figure 2. FTIR spectrum of (a) Tryp, (b) Tryp-IP before and (c) Tryp-IP after removal of the template and (d) NIP

SEM analysis

Figures 3(a) and 3(b) show the SEM micrographs for Tryp-IP and NIP, respectively. Bulky particles with the size in the range of a few microns is observed. This morphological feature is typical for polymers synthesized by the bulk polymerization approach. Furthermore, agglomeration is observed in Tryp-IP and NIP, and this is expected due to the high molar ratio of monomer to cross-linker (10:30) used in this study [24, 25]. Based on previous studies, bulk polymerization using the optimum molar ratio (4:20) can give a morphological image in heterogeneous irregular shapes and sizes due to crashing, grinding, and sieving processes [26]. Besides, the molar ratio of the cross-linker played a significant role in controlling the morphology of the polymer where it can form a rigid surface of the primary particles, which makes it difficult to agglomerate [27]. As in a previous study reported in the literature, the polymer morphology changes when the cross-linker ratio exceeds the optimum level within the polymer structure, resulting in the hard segment and a reduction in the polymer matrix binding sites [24].

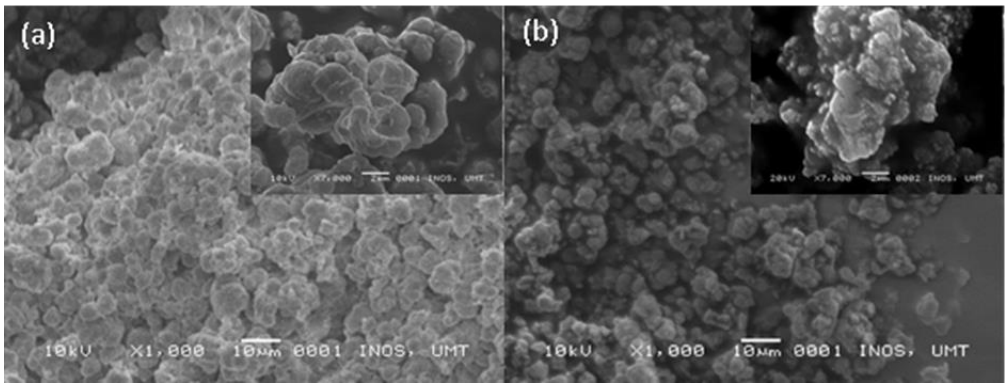

Figure 3. SEM micrograph of (a) Tryp-IP and (b) NIP

BET surface area analysis and porosity

BET analysis was carried out to determine the specific surface area and porosity properties of the Tryp-IP and NIP. Table 1 shows the results of surface area, pore volume and pore diameter of the polymers. The average pore diameters of Tryp-IP and NIP were in the range of 2–50 nm, indicating that both polymers have a mesoporous structure [20, 28]. However, Tryp-IP has larger a surface area and slightly larger total pore volume than the NIP. The increased surface area in Tryp-IP reflects the effect of the imprinting process, which occurred when the presence of the Tryp as a template during MIP synthesis resulted in the formation of pores or imprinted cavities [29, 30]. Based on previous studies, high molar ratios of monomers to the cross-linker resulted in non-specific interactions, while low ratios lead to inadequate functional sites [31]. Consequently, the agglomeration of the polymers particle resulted in the reduction of surface area and the number of active sites of polymers.

Table 1. BET surface area, pore volume and pore diameter

Polymer	Surface area ($m^2 g^{-1}$)	Pore volume ($cm^3 g^{-1}$)	Pore diameter (nm)
Tryp-IP	6.4519	0.022482	13.94
NIP	4.0351	0.016078	15.94

Adsorption isotherm study

The effect of the mass polymer was investigated to get the optimum mass for Tryp-IP. Based on Figure 4, it was observed that the percentage removal of Tryp increased with the increase of polymer mass. The maximum percentage removal achievable by Tryp-IP and NIP were 82% and 70%, respectively. An increase in polymer mass appears to increase the number of active sites and surface area for Tryp adsorption [32, 33]. Due to the absence of a template during the NIP synthesis, the non-specific cavities are formed, thus lower percentage removal of NIP than Tryp-IP. Based on Figure 4, the percentage removal increased until it reached the optimum level at 5 mg, indicating that all cavities were filled with Tryp molecules. However, a previous study agreed that a further increase in polymer mass could lead to adsorbent aggregation resulting in a decrease in the adsorption sites [34]. Hence, an increase in polymer mass does not increase the adsorption of Tryp.

Figure 5 is the isotherm models used in this study to fit the experimental data to predict the adsorption mechanism. Based on the isotherm parameter in Figures 5(a) and 5(b), the adsorption mechanism for Tryp-IP followed the Langmuir isotherm model and NIP followed the Redlich-Peterson isotherm which gave the highest R^2 value. The Langmuir isotherm was described as monolayer adsorption of Tryp onto Tryp-IP. The possible way for monolayer adsorption is for the adsorption to take place on the homogenous surface of the polymer matrix [35]. The similar observation was reported by the adsorption of D-Tryp onto polymer matrix [36]. To further strengthen the important features of the Langmuir isotherm model, the dimensionless constant separation factor (RL) was calculated [37]. RL values were found in the range of 0.017-0.009, which confirms adsorption of Tryp onto Tryp-IP was good. For the NIP, the data was fitted to the Redlich-Peterson model which, incorporates the features of both Langmuir and Freundlich isotherm. This can be applied as a homogeneous and heterogeneous system due to its versatility [38]. The parameters calculated for the three isotherms are tabulated in Table 2. From the data obtained, the maximum adsorption capacity for Tryp onto Tryp-IP was found to be 0.98 mg/g, which was seven times lower than the NIP (7.325 mg/g). The similar finding was reported by Hasanah et.al, which might be due to the non-specific recognition sites in NIP and therefore, made it swells better in polar solvent [39].

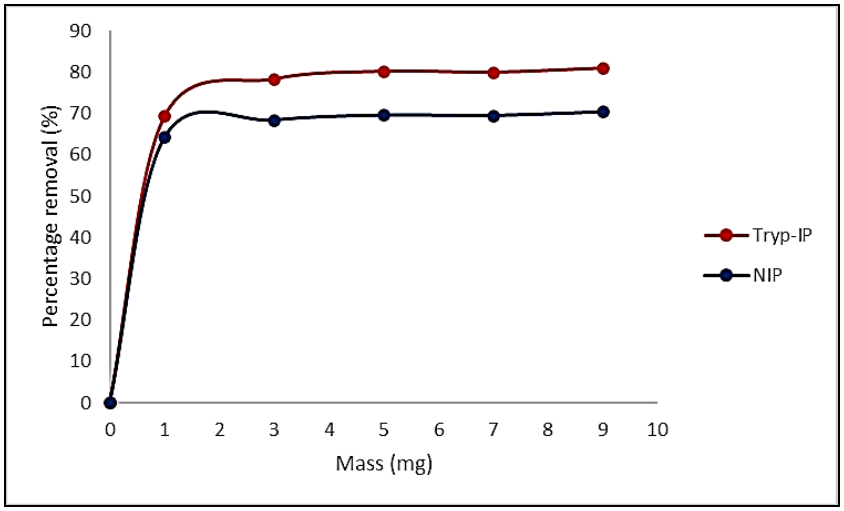

Figure 4. Effect of mass polymer on adsorption Tryp by Tryp-IP and NIP

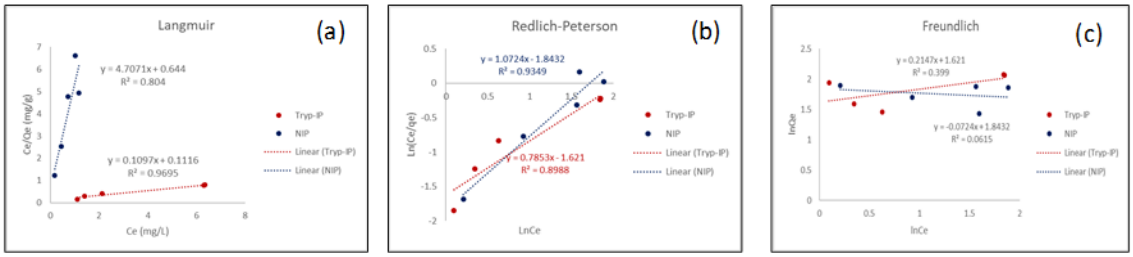

Figure 5. Adsorption isotherms of Tryp-IP and NIP using models (a) Langmuir (b) Redlich-Peterson (c) Freundlich

Table 2. Isotherm parameter for adsorption of Tryp by Tryp-IP and NIP

Polymer	Langmuir			Redlich-Peterson			Freundlich		
	Q_o	B	R^2	ß	A	R^2	1/n	K_F	R^2
Tryp-IP	0.98	9.116	0.9695	0.7853	5.058	0.8988	0.2147	5.058	0.399
NIP	7.325	0.212	0.804	1.0724	6.3167	0.9349	-0.0724	6.3167	0.0615

Adsorption kinetic study

The effect of contact time on the binding capacity of polymers is important to evaluate the binding efficiency in adsorption studies. It has been observed that the adsorption of Tryp onto the polymer surface increases with prolonging the contact time up to achieve equilibrium [40]. In Figure 6, initially, the adsorption rate of Tryp onto the polymeric surface was accelerating due to the abundant number of empty adsorption sites that can be accessed and less mass transfer resistance which allowed the active sites to capture the target analyte. However, with the progress of time, the number of active sites decreases, the imprinted cavities are gradually filled

with Tryp and the mass transfer resistance of Tryp to the active sites increases. Thus, the adsorption rate decreases and the removal percentage decreases slowly [41]. Finally, the adsorption equilibrium was reached within 120 min for Tryp-IP and 150 min for NIP. There is no change in the percentage removal if the time is prolonged because the polymer binding sites have been occupied with the Tryp. Therefore, it could be observed that Tryp-IP exhibited slightly higher percentage removal and faster mass transfer than the NIP, which could be attributed to the imprinting effect of Tryp [35, 42].

The adsorption mechanism was further evaluated by two of the most widely used kinetic models which is pseudo-first order kinetics, and pseudo-second order kinetic models. The results shown in Table 3 indicates that the R^2 value of Tryp-IP is most fitted with pseudo-second order (R^2 =0.9698) whereas the R^2 value for pseudo-first order is 0.2195. In the pseudo-second-order model, the theoretical and experimental adsorption capacity values were in good agreement. Therefore, the pseudo-second-order adsorption mechanism is predominant and the rate-limiting step at the surface involving a chemisorption process between Tryp and cavities of Tryp-IP [38].

Moreover, the values of Δq and RE were found to be low compared to pseudo-first order which means the accuracy and validity of the kinetic model were better equipped with pseudo second order. However, NIP appeared to be more suitable with pseudo-first order with the highest R^2 value (0.9107). It was expected that the rate of adsorption is proportional to the number of unused sites and the rate-limiting step was physisorption [39]. As in the case of Tryp-IP where Δq and RE values of NIP were exceedingly low for pseudo-first-order compared to pseudo-second order, these values indicate the accuracy of this kinetic model. Furthermore, the adsorption capacity Q_e (Table 3) for Tryp-IP (10.0336) was lower than NIP (11.3958). This result is due to the absence of specific recognition sites in the NIP, thus leading to the physical adsorption and random interaction of the Tryp molecule with the functional group of MAA in the polymer chain [43].

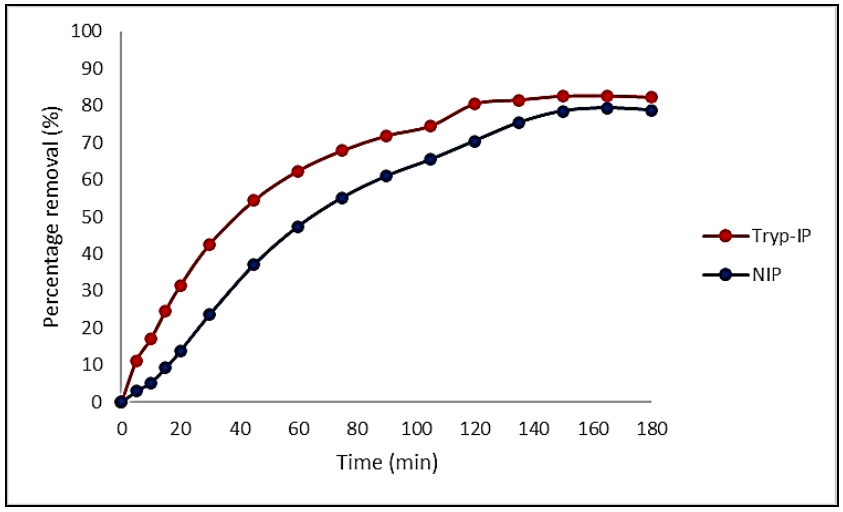

Figure 6. Effect of contact time on adsorption Tryp by Tryp-IP and NIP

Table 3. Kinetic parameter for adsorption of Tryp by Tryp-IP and NIP

Polymer	Model	Kinetic Parameters					
		y = mx + c	Q_e (mg/g)	Q_e (mg/g)	Δq (%)	RE (%)	R^2
Tryp-IP	Pseudo-first-order	y= -0.0223x +1.909	10.0336	6.746	8.464	32.78	0.2196
	Pseudo-second-order	y= 8.0813x +2.902		12.3001	5.826	22.56	0.9698
NIP	Pseudo-first-order	y= -0.017x +2.478	11.3958	11.9174	1.18	4.58	0.9107
	Pseudo-second-order	y= 0.0353x +7.9307		28.3286	38.37	149	0.3772

Effect pH study

The pH of the adsorption medium is the most critical parameter influencing the adsorption capacity [29]. In this analysis, a pH of 4-13 has been selected. Figure 7 shows that the highest percentage removal was obtained when the pH is in acidic condition and the percentage removal decreases as the pH increases (base condition). This condition might be due to the interaction of hydrogen bonding between the surface of the carboxylic group of MAA and the functional group of Tryp. As shown in Figure 7, the highest percentage removal of Tryp appeared when the pH became acidic. This observation occurred as a result of the zwitterionic Tryp and the large electronegativity of the oxygen atom of the carbonyl group in the polymers [43]. However, when the pH value becomes basic, Tryp exists as an anion and diffuses very slowly into the polymer surface [44]. Therefore, pH 5 was chosen as the optimal pH throughout this study.

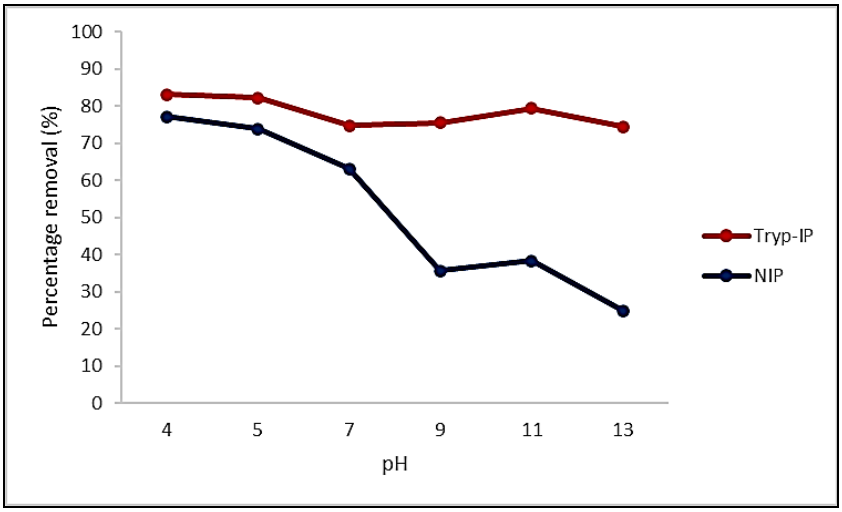

Figure 7. Effect of pH on adsorption Tryp by Tryp-IP and NIP

Effect of selectivity study

To study the selectivity of Tryp-IP and NIP, the recognition of Tryp was compared with tyrosine, phenylalanine and kynurenine as potential interferences. Table 4 shows the k_d values of each molecule in the Tryp-IP and the NIP. According to the Table 4, Tryp has higher k_d values compared to the other molecules in the Tryp-IP, which means that high specific recognition ability for Tryp is associated with a unique complementary form of the binding sites [42]. In contrast with the NIP, tyrosine gave a higher k_d value compared to Tryp. This is due to the non-specific

cavities existing in the NIP. Furthermore, the k values indicate that the polymer has selective behavior for the template in the presence of other molecules. The larger the k values, the higher the selectivity of the polymer towards the template compared to the other molecule [23]. For the Tryp-IP, the k values are higher than for the NIP, which means that Tryp-IP has selective behavior for Tryp as calculated in Equation 12. In order to show the efficiency of Tryp-IP for selective separation of Tryp against NIP, the k' values were calculated according to Equation 13. The larger the k' values the more selective is the Tryp-IP against NIP for the template toward the other molecules [41]. It can be concluded that the Try-IP has greater molecular recognition towards its template molecule.

Table 4. Selectivity study constant for Tryp-IP and NIP

	Tryp-IP		**NIP**		**k'**
	k_d	K	k_d	k	
Tryptophan	1.5751	-	1.2175	-	-
Kynurenine	0.7495	2.1015	0.8407	1.4482	1.451112
Tyrosine	0.5309	3.958	1.3346	0.9123	4.338485
Phenylalanine	0.8392	4.7168	0.7567	1.609	2.93151

Effect of the reproducibility study

The reproducibility performance of the Tryp-IP was evaluated by comparing the adsorption capacity for each adsorption process of Tryp-IP. The result in Figure 8 revealed that the percentage removal of Tryp did not show a significant change (80% to 83%) for each repeated usage. The Tryp-IP can be used at least nine times while maintaining its percentage removal of more than 80%, reflecting the excellent precision and reproducibility of the proposed polymer. Therefore, Tryp-IP showed good stability and could maintain its adsorption capacity at a constant value.

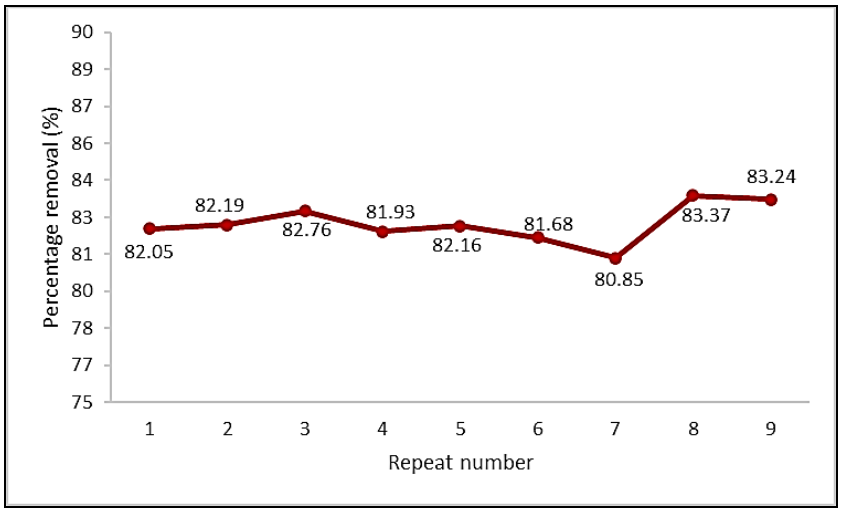

Figure 8. Effect of reproducibility of Tryp-IP

Conclusion

In this study, Tryp-IP and NIP were successfully synthesized through bulk polymerization and used as an adsorbent for tryptophan detection. FTIR, SEM, and BET were used to analyze the physical and chemical characterizations, which revealed evidence of chemical interaction, surface morphology, and cavities of the polymer matrix; all of which are responsible for the binding ability of the polymer. Hence, the adsorption studies have revealed that Tryp-IP has a greater removal percentage, selectivity, and stability than the NIP.

Acknowledgments

We would like to thank the Ministry of Higher Education Malaysia for the project funding support under Fundamental Research Grant Scheme (FRGS/1/2018/STG01/UMT/02/6 – Vot: 59493) and Universiti Malaysia Terengganu.

References

1. Friedman, M. (2018). Analysis, nutrition, and health benefits of tryptophan. *International Journal of Tryptophan Research*, 11: 1178646918802282.
2. Richard, D. M., Dawes, M. A., Mathias, C. W., Acheson, A., Hill-Kapturczak, N. and Dougherty, D. M. (2009). L-tryptophan: basic metabolic functions, behavioral research and therapeutic indications. *International Journal of Tryptophan Research*, 23(2): 45-60.
3. Lindseth, G., Helland, B. and Caspers, J. (2015). The effects of dietary tryptophan on affective disorders. *Archives of Psychiatric Nursing*, 29(2): 102-107.
4. Jenkins, T. A., Nguyen, J. C. D., Polglaze, K. E. and Bertrand, P. P. (2016). Influence of tryptophan and serotonin on mood and cognition with a possible role of the gut-brain axis. *Nutrients*, 8(1): 56.
5. Sundaresan, R., Mariyappan, V., Chen, S.-M., Keerthi, M. and Ramachandran, R. (2021). Electrochemical sensor for detection of tryptophan in the milk sample based on $MnWO_4$ nanoplates encapsulated RGO nanocomposite. *Colloids and Surfaces A: Physicochemical and Engineering Aspects*, 625: 126889.
6. Capuron, L., Ravaud, A., Neveu, P. J., Miller, A. H., Maes, M. and Dantzer, R. (2002). Association between decreased serum tryptophan concentrations and depressive symptoms in cancer patients undergoing cytokine therapy. *Molecular Psychiatry*, 7(5): 468-473.
7. de Jong, R. A., Nijman, H. W., Boezen, H. M., Volmer, M., Klaske, A., Krijnen, J., van der Zee, A. G. J., Hollema, H. and Kema, I. P. (2011). Serum tryptophan and kynurenine concentrations as parameters for indoleamine 2, 3-dioxygenase activity in patients with endometrial, ovarian, and vulvar cancer. *International Journal of Gynecologic Cancer*, 21(7): 1320-1327.
8. Onesti, C. E., Boemer, F., Josse, C., Leduc, S., Bours, V. and Jerusalem, G. (2019). Tryptophan catabolism increases in breast cancer patients compared to healthy controls without affecting the cancer outcome or response to chemotherapy. *Journal of Translational Medicine*, 17(1): 1-11.
9. Tian, Y., Deng, P., Wu, Y., Ding, Z., Li, G., Liu, J. and He, Q. (2019). A simple and efficient molecularly imprinted electrochemical sensor for the selective determination of tryptophan. *Biomolecules*, 9(7): 294.
10. Jiao, P., Wei, Y., Zhang, M., Zhang, X., Zhang, H. and Yuan, X. (2021). Adsorption separation of l-tryptophan based on the hyper-cross-linked resin XDA-200. *ACS Omega*, 6(3): 2255-2263.
11. Lee, D., Hussain, S., Yeo, J. and Pang, Y. (2021). Adsorption of dipeptide L-alanyl-L-tryptophan on gold colloidal nanoparticles studied by surface-enhanced Raman spectroscopy. *Spectrochimica Acta Part A: Molecular and Biomolecular Spectroscopy*, 247: 119064.
12. Belhamdi, B., Merzougui, Z., Laksaci, H. and Trari, M. (2019). The removal and adsorption mechanisms of free amino acid l-tryptophan from aqueous solution by biomass-based activated carbon by H_3PO_4 activation: regeneration study. *Physics and Chemistry of the Earth, Parts A/B/C*, 114: 102791.

13. Mehamod, F. S., KuBulat, K., Yusof, N. F. and Othman, N. A. (2015). The development of molecular imprinting technology for caffeine extraction. *International Journal of Technology*, 6(4): 546-554.
14. Samarth, N. B., Kamble, V., Mahanwar, P. A., Rane, A. V. and Abitha, V. K. (2015). A historical perspective and the development of molecular imprinting polymer-A review. *Chemistry International*, 4: 202-210.
15. Mujahid, A. and Dickert, F. L. (2016). Molecularly Imprinted polymers: principle, design, and enzyme-like catalysis. *Molecularly Imprinted Catalysts: Principles, Syntheses, and Applications*, pp. 79-101.
16. Zhang, H., Ye, L. and Mosbach, K. (2006). Non-covalent molecular imprinting with emphasis on its application in separation and drug development. *Journal of Molecular Recognition: An Interdisciplinary Journal*, 19(4), 248-259.
17. Yusof, N. F., Mehamod, F. S., Kadir, M. A. and Suah, F. B. M. (2018). Characteristics of adsorption isotherm and kinetic study for newly prepared Co2+-imprinted polymer linkage with dipicolinic acid. *IOP Conference Series: Materials Science and Engineering*, 440(1): 012005.
18. Yusof, N. F., Mehamod, F. S. and Suah, F. B. M. (2018). The effect of RAFT polymerization on the physical properties of thiamphenicol-imprinted polymer. *E3S Web of Conferences*, 67(12): 03050.
19. Abdul Hamid, N. S., Naseeruteen, F., Wan Ngah, W. S., Yusof, N. F., Mehamod, F. S. and Mohd Suah, F. B. (2020). Synthesis of chitin-ionic liquid beads as potential adsorbents for methylene blue. *Malaysian Journal of Chemistry*, 22(2): 98-110.
20. Yusof, N. F., Mehamod, F. S. and Suah, F. B. M. (2019). Fabrication and binding characterization of ion imprinted polymers for highly selective Co2+ ions in an aqueous medium. *Journal of Environmental Chemical Engineering*, 7(2): 103007.
21. Ayawei, N., Ebelegi, A. N. and Wankasi, D. (2017). Modelling and interpretation of adsorption isotherms. *Journal of Chemistry*, 2017: 3039817.
22. Alveroglu, E., Balouch, A., Khan, S., Mahar, A. M., Jagirani, M. S. and Pato, A. H. (2021). Evaluation of the performance of a selective magnetite molecularly imprinted polymer for extraction of quercetin from onion samples. *Microchemical Journal*, 162: 105849.
23. Fareghi, A. R., Moghadam, P. N., Khalafy, J., Bahram, M. and Moghtader, M. (2017). Preparation of a new molecularly imprinted polymer based on self-crosslinkable cellulose acrylate in aqueous solution: A drug delivery system for furosemide. *Journal of Applied Polymer Science*, 134(48): 45581.
24. Prabakaran, K., Jandas, P. J., Luo, J., Fu, C. and Wei, Q. (2021). Molecularly imprinted poly (methacrylic acid) based QCM biosensor for selective determination of L-tryptophan. *Colloids and Surfaces A: Physicochemical and Engineering Aspects*, 611: 125859.
25. Azodi-Deilami, S., Abdouss, M. and Seyedi, S. R. (2010). Synthesis and characterization of molecularly imprinted polymer for controlled release of tramadol. *Central European Journal of Chemistry*, 8(3): 687-695.
26. Wang, L., Zhi, K., Zhang, Y., Liu, Y., Zhang, L., Yasin, A. and Lin, Q. (2019). Molecularly imprinted polymers for gossypol via sol–gel, bulk, and surface layer imprinting—a comparative study. *Polymers*, 11(4): 602.
27. Xia, Q., Yun, Y., Li, Q., Huang, Z. and Liang, Z. (2017). Preparation and characterization of monodisperse molecularly imprinted polymer microspheres by precipitation polymerization for kaempferol. *Designed Monomers and Polymers*, 20(1): 201-209.
28. Madikizela, L. M., Zunngu, S. S., Mlunguza, N. Y., Tavengwa, N. T., Mdluli, P. S. and Chimuka, L. (2018). Application of molecularly imprinted polymer designed for the selective extraction of ketoprofen from wastewater. *Water SA*, 44(3): 406-418.
29. Hasanah, A. N., Susanti, I., Marcellino, M., Maranata, G. J., Saputri, F. A. and Pratiwi, R. (2021). Microsphere molecularly imprinted solid-phase extraction for diazepam analysis using itaconic acid as a monomer in propanol. *Open Chemistry*, 19(1): 604-613.

30. Yusof, N. F., Mehamod, F. S., & Suah, F. B. M. (2020). Adsorptive removal of bis (2-ethylhexyl) phthalate using an imprinted polymer: isotherm and kinetic modelling. *International Journal of Environmental Analytical Chemistry*, 2020: 1-12.
31. Song, S., Wu, A., Shi, X., Li, R., Lin, Z. and Zhang, D. (2008). Development and application of molecularly imprinted polymers as solid-phase sorbents for erythromycin extraction. *Analytical and Bioanalytical Chemistry*, 390(8): 2141-2150.
32. Albadarin, A. B., Mangwandi, C., Ala'a, H., Walker, G. M., Allen, S. J. and Ahmad, M. N. M. (2012). Kinetic and thermodynamics of chromium ions adsorption onto low-cost dolomite adsorbent. *Chemical Engineering Journal*, 179: 193-202.
33. Gomes, C., Sadoyan, G., Dias, R. and Costa, M. R. P. F. N. (2017). Development of molecularly imprinted polymers to target polyphenols present in plant extracts. *Processes*, 5(4): 72.
34. Mor, S., Chhoden, K. and Ravindra, K. (2016). Application of agro-waste rice husk ash for the removal of phosphate from the wastewater. *Journal of Cleaner Production*, 129: 673-680.
35. Bakhtiar, S., Bhawani, S. A. and Shafqat, S. R. (2019). Synthesis and characterization of molecular imprinting polymer for the removal of 2-phenylphenol from spiked blood serum and river water. *Chemical and Biological Technologies in Agriculture*, 6(1): 1-10.
36. Jin, Y., Liu, C. C., Sun, X. H., Lee, K. J., Jung, Y. A. and Row, K. H. (2012). Adsorption isotherms of tryptophan enantiomer on d-tryptophan molecular imprinted polymer. *Asian Journal of Chemistry*, 24(6): 2461-2466.
37. Hameed, B. H., Ahmad, A. L. and Latiff, K. N. A. (2007). Adsorption of basic dye (methylene blue) onto activated carbon prepared from rattan sawdust. *Dyes and Pigments*, 75(1): 143-149.
38. Kumar, V. (2019). Adsorption kinetics and isotherms for the removal of rhodamine B dye and Pb^{2+} ions from aqueous solutions by a hybrid ion-exchanger. *Arabian Journal of Chemistry*, 12(3): 316-329.
39. Hasanah, A. N., Dwi Utari, T. N. and Pratiwi, R. (2019). Synthesis of atenolol-imprinted polymers with methyl methacrylate as functional monomer in propanol using bulk and precipitation polymerization method. *Journal of Analytical Methods in Chemistry*, 2019: 9853620.
40. Yusof, N. F., Mehamod, F. S., Jusoh, N., Amin, K. A. M. and Suah, F. B. M. (2017). Ion-imprinted polymer-based on picolinic acid as a co-functional monomer for highly selective sorption of Cu(II) ions in an aqueous solution. *AIP Conference Proceedings*, 1885: 020017.
41. Abouzarzadeh, A., Forouzani, M., Jahanshahi, M. and Bahramifar, N. (2012). Synthesis and evaluation of uniformly sized nalidixic acid–imprinted nanospheres based on precipitation polymerization method for analytical and biomedical applications. *Journal of Molecular Recognition*, 25(7): 404-413.
42. Pan, J., Li, L., Hang, H., Ou, H., Zhang, L., Yan, Y. and Shi, W. (2013). Study on the nonylphenol removal from aqueous solution using magnetic molecularly imprinted polymers based on fly-ash-cenospheres. *Chemical Engineering Journal*, 223: 824-832.
43. Kong, Y., Zhao, W., Yao, S., Xu, J., Wang, W. and Chen, Z. (2010). Molecularly imprinted polypyrrole prepared by electrodeposition for the selective recognition of tryptophan enantiomers. *Journal of Applied Polymer Science*, 115(4), 1952-1957.
44. Monier, M., Abdel-Latif, D. A. and Nassef, H. M. (2015). Preparation of l-tryptophan imprinted microspheres based on carboxylic acid functionalized polystyrene. *Journal of Colloid and Interface Science*, 445: 371-379.